

General Disclaimer

One or more of the Following Statements may affect this Document

- This document has been reproduced from the best copy furnished by the organizational source. It is being released in the interest of making available as much information as possible.
- This document may contain data, which exceeds the sheet parameters. It was furnished in this condition by the organizational source and is the best copy available.
- This document may contain tone-on-tone or color graphs, charts and/or pictures, which have been reproduced in black and white.
- This document is paginated as submitted by the original source.
- Portions of this document are not fully legible due to the historical nature of some of the material. However, it is the best reproduction available from the original submission.

Radar Error Statistics for the Space Shuttle

(NASA-TM-80508) RADAR ERROR STATISTICS FOR
THE SPACE SHUTTLE (NASA) 22 p HC A02/MF A01
CSCL 17I

N79-30279

Unclass
G3/16 31941



Mission Planning and Analysis Division

July 1979



National Aeronautics and
Space Administration

Lyndon B. Johnson Space Center
Houston, Texas

SHUTTLE PROGRAM

RADAR ERROR STATISTICS
FOR THE SPACE SHUTTLE

By William M. Lear, TRW

Approved: Emil R. Schiesser
Emil R. Schiesser, Chief
Mathematical Physics BranchApproved: Ronald L. Berry
Ronald L. Berry, Chief
Mission Planning and Analysis Division

Mission Planning and Analysis Division
National Aeronautics and Space Administration
Lyndon B. Johnson Space Center
Houston, Texas
July 1979

CONTENTS

Section		Page
1.0	<u>INTRODUCTION</u>	1
2.0	<u>C-BAND ERROR STATISTICS</u>	1
3.0	<u>S-BAND ERROR STATISTICS</u>	8
4.0	<u>REFERENCES</u>	15

PRECEDING PAGE BLANK NOT FILMED

TABLES

Table	Page
I σ_{qp} , σ_{qA} AND σ_{qE} FOR $H = 2 \cdot 10^5$ METERS	3
II σ_{Bp} , σ_{BA} , σ_{BE} FOR $H = 2 \cdot 10^5$ METERS	6

FIGURES

1.0 INTRODUCTION

This report presents C-band and S-band radar error statistics that are recommended for use with the groundtracking programs used to process Space Shuttle tracking data. The statistics are divided into two parts: bias error statistics, using the subscript B, and high-frequency error statistics, using the subscript q. Bias errors may be slowly varying to constant. High-frequency random errors (noise) are rapidly varying and may or may not be correlated from sample to sample.

Bias errors are mainly due to hardware defects and to errors in correction for atmospheric refraction effects. High-frequency noise is mainly due to hardware and due to atmospheric "scintillation". This report identifies three types of atmospheric scintillation: horizontal, vertical, and line of sight. This is the first time that horizontal and line-of-sight scintillations have been identified.

2.0 C-BAND ERROR STATISTICS

The C-band error statistics apply to the following radars: FPS-16, TPQ-18, FPQ-6, FPQ-13, FPQ-14, and FPQ-15. Hardware error statistics for the C-band radars for the Eastern Test Range were obtained from references 1, 2, and 3, which gave results based on 9 months of tracking data. Hardware error statistics for the Western Test Range C-band radars were obtained from reference 4, which gave results based on 13 months of tracking data. Differences between Eastern Test Range and Western Test Range statistics were small. Also, all the various radars seemed to have about the same statistics. Note though that some radars can track at longer ranges than others.

The table below lists the hardware error statistics, subscript H. The symbol σ_q denotes high-frequency error standard deviation. The symbol σ_B denotes the bias error standard deviation. Subscripts ρ , A, E denote range, azimuth angle, and elevation angle. Maximum and minimum values of σ are also shown. These are the extreme values observed among the 15 tracking sites used to determine the average (RMS) statistics and are generally based on several tracking passes. Larger or smaller values may occur for any individual pass of tracking data. There also seemed to be little difference between the small amount of skin tracking data statistics and the beacon tracking statistics. An exception was $\sigma_{B\rho}$, which seemed to be less. The $\sigma_{B\rho}$ for beacon tracking was larger, probably due to unknown time delays in the beacon, and is the one shown in the following table.

$\sigma_{q\rho H} = 2.7 \text{ m}$	$\sigma_{q\rho H, \text{MAX}} = 4.9 \text{ m}$	$\sigma_{q\rho H, \text{MIN}} = 1.0 \text{ m}$
$\sigma_{qAH} = 0.10 \text{ mrad}$	$\sigma_{qAH, \text{MAX}} = 0.14 \text{ mrad}$	$\sigma_{qAH, \text{MIN}} = 0.07 \text{ mrad}$
$\sigma_{qEH} = 0.11 \text{ mrad}$	$\sigma_{qEH, \text{MAX}} = 0.15 \text{ mrad}$	$\sigma_{qEH, \text{MIN}} = 0.07 \text{ mrad}$
$\sigma_{B\rho H} = 12.5 \text{ m}$	$\sigma_{B\rho H, \text{MAX}} = 17.4 \text{ m}$	$\sigma_{B\rho H, \text{MIN}} = 7.9 \text{ m}$
$\sigma_{BAH} = 0.08 \text{ mrad}$	$\sigma_{BAH, \text{MAX}} = 0.11 \text{ mrad}$	$\sigma_{BAH, \text{MIN}} = 0.05 \text{ mrad}$
$\sigma_{BEH} = 0.12 \text{ mrad}$	$\sigma_{BEH, \text{MAX}} = 0.21 \text{ mrad}$	$\sigma_{BEH, \text{MIN}} = 0.05 \text{ mrad}$

The errors listed in the preceding table are the dominant errors for elevation angles above 5 degrees. At low-elevation angles, σ_q is increased because of atmospheric scintillation noise. The magnitude of the scintillation noise is dependent on the amount of atmosphere between the tracker and the target. The parameter a is used to quantify this amount of atmosphere and is defined below.

$\Delta\rho$ = range refraction correction

$$\Delta\rho = \rho_{\text{MEASURED}} - \rho_{\text{GEOMETRIC}} \quad (1)$$

$$R_o = 1 \text{ Earth radius} = 6378165 \text{ m}$$

$$a = \sqrt{1 - \exp(-(10^5 \Delta\rho / R_o)^4)} \quad (2)$$

$\Delta\rho$ has an approximate range of values of

$$0 \leq \Delta\rho < 144 \text{ m}$$

The parameter a ranges from zero to one. The symbol $a = 0$ means little atmosphere between the tracker and target. The $a = 1$ means a large amount of atmosphere. The a is small, $a < .13$, for $E > 5$ degrees.

To obtain the total σ_q for the high-frequency noise, the hardware noise is root sum squared with the scintillation noise in the following manner.

$$\sigma_q = \sqrt{\sigma_{qH}^2 + (a\sigma_{qS})^2} \quad (3)$$

Based on personal analysis of low-elevation angle S-band data, the scintillation standard deviations are

$$\sigma_{qPS} = 0.005 \text{ meters}$$

$$\sigma_{qAS} = 0.15 \text{ mrad}$$

$$\sigma_{qES} = 0.5 \text{ mrad}$$

References 1, 2, and 3 also indicate a value of σ_{qES} of 0.5 mrad. Using the root mean square (RMS) σ_{qH} errors (left column), a table of σ_{qP} , σ_{qA} and σ_{qE} versus E_{MEASURED} (table I) has been constructed using a modulus of refraction of $N_0 = 0.000395$ and an orbital altitude of 108 n. mi.

TABLE I.- σ_{q_p} , σ_{q_A} AND σ_{q_E} FOR $H = 2 \cdot 10^5$ METERS

E_M , deg	σ_{q_p} , m	σ_{q_A} , mrad	σ_{q_E} , mrad
0	2.7	0.18	0.51
.1	2.7	.18	.51
.2	2.7	.18	.51
.3	2.7	.18	.51
.4	2.7	.18	.51
.5	2.7	.18	.51
.7	2.7	.18	.50
1	2.7	.17	.47
2	2.7	.13	.29
3	2.7	.11	.19
4	2.7	.10	.15
5	2.7	.10	.13
7	2.7	.10	.12
10	2.7	.10	.11

Low-elevation angle tracking also causes an increase in the range and elevation angle bias error standard deviations. This increase is because of errors in correcting for refraction effects. These errors can be quite large. Two sources of refraction errors are identified. The first is the error in the estimate of the modulus of refraction N_0 at the observer (station). For Space Shuttle tracking, mean monthly values of N_0 will be used. A study of reference 5 reveals that N_0 is changed from month to month by an average amount of 1.7 percent with a maximum change of 7.5 percent observed at one station. It is not meant to imply that using mean monthly averages is bad. In fact, they may represent the total atmosphere above the station better than an estimate made near the track time. Note that diurnal variations in N_0 at inland stations may be as much as 6 percent from the mean daily value. A strong weather front passage can change N_0 by 14 percent. Thus, a 1σ error in N_0 of 2.5 percent is suggested for use with Space Shuttle tracking. That is,

$$\sigma_{N0}/N_0 = 0.025$$

Using the equations of reference 6 for low-elevation angles and high altitudes, the following approximations can be made. The bias error standard deviation for range, due to errors in N_0 , is approximately

$$\sigma_{BpN} = 0.5(\sigma_{N0}/N_0)\Delta\rho \quad (4)$$

And for elevation angle

$$\sigma_{BEN} = (\sigma_{N0}/N_0)\Delta E \quad (5)$$

where $\Delta\rho$ and ΔE are the computed refraction corrections.

Another major source of bias error due to refraction effects is in the algorithms used to compute $\Delta\rho$ and ΔE . These algorithm standard deviations are denoted by σ_{BpA} and σ_{BEA} . The accuracy of any particular algorithm may be checked using the extensive tables of "exact" corrections in reference 6. Even very precise algorithms will contain some error because of the assumptions made about the atmosphere, namely that the modulus of refraction N decreases exponentially with increasing altitude, and that the Earth is spherical in the vicinity of the tracker. The assumption error may be on the order of 1 percent of the computed correction. The best algorithm for ΔE in reference 6 had a maximum error of 41 percent for $E = 0^\circ$. At $E = 2^\circ$ the maximum error was 5.85 percent for low altitudes and 1.6 percent at high altitudes. The best algorithm for $\Delta\rho$ in reference 6 had an overall accuracy of 1.6 percent. In reference 7, the best algorithm for ΔE had an overall accuracy of 1.7 percent. Reference 8 gives refraction correction algorithms for altitudes above 54 n. mi. Here, $\Delta\rho$ had an accuracy of 0.44 percent and ΔE had an accuracy of 0.55 percent.

Thus, the total bias error standard deviations are

$$\sigma_{Bp} = \sqrt{\sigma_{BpH}^2 + \sigma_{BpN}^2 + \sigma_{BpA}^2} \quad (6)$$

$$\sigma_{BA} = \sigma_{BAH} \quad (7)$$

$$\sigma_{BE} = \sqrt{\sigma_{BEH}^2 + \sigma_{BEN}^2 + \sigma_{BEA}^2} \quad (8)$$

Let

$$\sigma_{B_0 H} = 12.5 \text{ m}$$

$$\sigma_{B_0 N} = 0.0125 \Delta \rho$$

$$\sigma_{B_0 A} = 0.02 \Delta \rho$$

$$\sigma_{BA} = \sigma_{BAH} = 0.08 \text{ mrad}$$

$$\sigma_{BEH} = 0.12 \text{ mrad}$$

$$\sigma_{BEN} = 0.025 \Delta E$$

$$\sigma_{BEA} = 0.02 \Delta E$$

Table II shows the total bias error standard deviations for $N_0 = 0.000395$ and $H = 108$ n. mi. It is seen that range and azimuth bias errors are little affected by refraction errors. σ_{BE} is strongly affected by refraction errors for $E_M < 5$ degrees.

TABLE II.- σ_{Bp} , σ_{BA} , σ_{BE} for $H = 2 \cdot 10^5$ METERS

E_M , deg	σ_{Bp} , m	σ_{BA} , mrad	σ_{BE} , mrad
0	12.9	0.08	0.63
.1	12.9	.08	.59
.2	12.8	.08	.56
.3	12.8	.08	.53
.4	12.7	.08	.50
.5	12.7	.08	.48
.7	12.7	.08	.44
1	12.6	.08	.39
2	12.6	.08	.28
3	12.5	.08	.23
4	12.5	.08	.20
5	12.5	.08	.18
7	12.5	.08	.15
10	12.5	.08	.14
20	12.5	.08	.12

Little is known about the autocorrelation function of the high-frequency noise adding to ρ , A and E . From reference 9, it appears that the range noise is essentially uncorrelated at 10 samples/second. However, the noise adding to azimuth and elevation angle is correlated at this sample rate. Exponential correlation is generally assumed with a time constant of $\tau \approx 2$ seconds. The autocorrelation functions is defined by

$$\phi_j = E(\epsilon_i \epsilon_{i-j}) = E(\epsilon(t_i) \epsilon(t_i - j\Delta T)) \quad (9)$$

$$E(\epsilon_i) = 0$$

Note $\phi_0 = E(\epsilon_i^2) = \sigma_q^2$ is the variance of ϵ_i , independent of the sample rate. Let

$$b = e^{-\Delta T/\tau} \quad (10)$$

where ΔT is the sample interval and τ is called the time constant. Simulated exponentially correlated noise is generated in the following manner (ref. 10)

$$E(n_i) = 0 \quad (11)$$

$$\begin{aligned} E(n_i n_j) &= 0 \quad \text{for } i \neq j \\ &= 1 \quad \text{for } i = j \end{aligned} \quad (12)$$

$$\epsilon_i = b\epsilon_{i-1} + \sigma_q \sqrt{1 - b^2} n_i \quad (13)$$

It can be shown now that the autocorrelation function of ϵ is given by

$$\phi_j = \sigma_q^2 b^j = \phi_0 \exp(-j\Delta T/\tau) \quad (14)$$

Thus the name exponentially correlated random variable, ECRV. Also note that $E(\epsilon_i) = 0$, it is a zero mean random variable.

Let us briefly obtain a further insight of the meaning of ϕ_j . In the absence of any information about ϵ_i , the best guess of its value is zero with an error of σ_q in the guess. That is

$$\epsilon_i = 0 \quad \pm \sigma_q \quad (15)$$

Now suppose that ϵ_{i-j} is given. Then it can be shown (ref. 10) that the new best estimate of ϵ_i is

$$\epsilon_i = (\phi_j/\phi_0)\epsilon_{i-j} \quad \pm \sigma_q \sqrt{1 - (\phi_j/\phi_0)^2} \quad (16)$$

For example, consider $\phi_j/\phi_0 < 0.4$. Then the 1 σ error is

$$\sigma_q \sqrt{1 - (\phi_j/\phi_0)^2} > 0.92\sigma_q \quad (17)$$

That is, the reduction in the uncertainty is less than 8 percent. Therefore, values of ϕ_j/ϕ_0 of less than 0.4 may be considered insignificant in this case.

3.0 S-BAND ERROR STATISTICS

S-band data consist of four measurements: range ρ ; X angle α_X ; Y angle α_Y ; and integrated Doppler data. The subscript D is used for integrated Doppler data that is equivalent to a range measurement plus a large bias (constant of integration). Integrated Doppler data have units of cycles. The conversion factor to meters is approximately 15 261 cycles/meter, or 15 cycles/mm.

All the error statistics were obtained from many passes of satellite tracking at various stations. The high frequency error statistics σ_{qp} will be considered first. These errors are due to atmospheric scintillation and to hardware errors that are the dominant errors for high-elevation angles. σ_{qXH} and σ_{qYH} were obtained by sliding, second-order, polynomial fits to 10-second data arcs (201 points) using a total of 2201 points. The midpoint fit value was compared to the raw data to obtain the error value. Many passes of 2201 points were used. A maximum of 2000 midpoint errors were obtained from these passes, from which the autocorrelation function for the X and Y angles were obtained. This work was performed under the direction of I. M. Salzburg, head of Orbit Operations Section, Operational Orbit Support Branch, Goddard Space Flight Center, but has not yet been published. W. Lear reduced the raw autocorrelation functions to an analytical form, determined the high-frequency range and Doppler statistics from raw satellite tracking data supplied by Goddard, and determined low-elevation angle statistics ($E \leq 5$ degrees). Second-order polynomial fits to 51-point samples were used for the angle data to generate error residuals. Third-order polynomials were necessary for the range and Doppler data.

The random noise sigma for the S-band range measurements, obtained by the author from Goddard data, is summarized below versus measured elevation angle.

E_M , degrees	1.1	1.5	2.0	2.5	3.0	3.5	4.0	4.5	5.0	
σ_{qp} , meters	.33	.36	.43	.50	.43	.41	.41	.41	.45	

σ_{qp} appeared to be independent of elevation angle; i.e., scintillation effects, σ_{qpS} , were small. The RMS value of the range noise was 0.43 meters with a maximum value 0.69 meters and a minimum value of 0.24 meters. Forty two 51-point samples were used. However, reference 11 indicates that the Space Shuttle S-band transponder may be more noisy than indicated above. The hardware theoretical value is 10 meters, 3σ . Thus, for the Shuttle

$$\sigma_{qpH} = 3.3 \text{ meters}$$

For the scintillation error (obtained below from the integrated Doppler data)

$$\sigma_{qpS} = 0.005 \text{ meters}$$

$$\sigma_{q\rho} = \sqrt{\sigma_{q\rho H}^2 + (a\sigma_{q\rho S})^2} = 3.3 \text{ meters} \quad (18)$$

where a is given by equation 2.

Reducing raw integrated Doppler data, the following was obtained by the author.

E_M , degrees	1.1	1.5	2.0	2.5	3.0	3.5	4.0	4.5	5.0
σ_{qD} , mm	5.0	4.0	3.2	3.1	2.5	2.4	2.6	1.8	1.5
	!	!	!	!	!	!	!	!	!

Thirty eight batches of 51-point data were used to obtain the values in the above table. To convert millimeters to cycles, multiply the above values by 15 cycles/mm. The above figures suggest a hardware value of $\sigma_{qDH} = 1.5$ mm; however, vibration effects may be larger than this. References 12, 13 and 14 list RMS residual values for least-squares orbit determinations. The residuals are due to random noise, bias errors, and fit errors and thus represent an upper bound for the Doppler noise statistics. The reference values gave $\sigma_{qDH} = 8$ mm, $\sigma_{qDH,MAX} = 12.7$ mm and $\sigma_{qDH,MIN} = 5$ mm. Conversely, five batches in the authors analysis showed $\sigma_{qDH} \leq .9$ mm; they were removed from the tabular statistics above. Thus, it is suggested

$$\sigma_{qDH} = 4 \text{ mm} = 60 \text{ cycles}$$

$$\sigma_{qDS} = 5 \text{ mm} = 75 \text{ cycles}$$

The total standard deviation is thus

$$\sigma_{qD} = \sqrt{\sigma_{qDH}^2 + (a\sigma_{qDS})^2} \quad (19)$$

$$\leq 6.4 \text{ mm} = 96 \text{ cycles}$$

And, for the S-band station in Hawaii at Kauai, HAW3, it is recommended (ref. 15)

$$\sigma_{qDH} = 24 \text{ mm} = 360 \text{ cycles}$$

For the 10 samples/second data, it was found by the author that the range noise had

$$\phi_1/\phi_0 = 0.4 \text{ (not strongly correlated)}$$

For the integrated Doppler data

$$\phi_1/\phi_0 = 0.2 \text{ (essentially uncorrelated)}$$

Based on Goddard's reduction of the S-band angle data

$$\sigma_{qXH} = 0.15 \text{ mrad} \quad \sigma_{qXH,MAX} = 0.40 \text{ mrad} \quad \sigma_{qXH,MIN} = 0.03 \text{ mrad}$$

$$\sigma_{qYH} = 0.09 \text{ mrad} \quad \sigma_{qYH,MAX} = 0.16 \text{ mrad} \quad \sigma_{qYH,MIN} = 0.04 \text{ mrad}$$

The above figures are based on 29 batches of 2201 raw data points. The angle data rate was 20 samples/second.

Both X and Y, angles are affected by scintillation error. The scintillation error is root sum squared with the hardware error in the following manner.

$$\sigma_{qX} = \sqrt{\sigma_{qXH}^2 + (a(\partial\alpha_X/\partial E)\sigma_{qES})^2 + (a(\partial\alpha_X/\partial A)\sigma_{qAS})^2} \quad (20)$$

$$\sigma_{qY} = \sqrt{\sigma_{qYH}^2 + (a(\partial\alpha_Y/\partial E)\sigma_{qES})^2 + (a(\partial\alpha_Y/\partial A)\sigma_{qAS})^2} \quad (21)$$

where (ref. 16)

$$\frac{\partial\alpha_X}{\partial E} = \frac{-\sin\alpha_X/\cos\alpha_Y}{\cos^2\alpha_X \sin^2\alpha_Y + \sin^2\alpha_X} \quad -8 < \frac{\partial\alpha_X}{\partial E} < 8 \text{ for } E \text{ small}$$

$$\frac{\partial\alpha_X}{\partial A} = \cos\alpha_X \sin\alpha_Y/\cos\alpha_Y \quad = 0 \text{ for } E = 0$$

$$\frac{\partial\alpha_Y}{\partial E} = \frac{-\cos\alpha_X \sin\alpha_Y}{\cos^2\alpha_X \sin^2\alpha_Y + \sin^2\alpha_X} \quad = 0 \text{ for } E = 0$$

$$\frac{\partial\alpha_Y}{\partial A} = -\sin\alpha_X \quad = \pm 1 \text{ for } E = 0$$

$$E = \arcsin(\cos\alpha_X \cos\alpha_Y)$$

Because the partials are multiplied by a , which is zero for large E , it may be approximated

$$\partial \alpha_X / \partial A = \partial \alpha_Y / \partial E = 0$$

$$\partial \alpha_Y / \partial A = 1$$

Analysis by the author of low-elevation angle S-band data shows:

$$\sigma_{qAS} = 0.15 \text{ mrad}$$

$$\sigma_{qES} = 0.5 \text{ mrad}$$

Note that at low-elevation angles, σ_{qAS} represents a horizontal scintillation and σ_{qES} represents a vertical scintillation, while σ_{qoS} and σ_{qDS} represent scintillation along the line of sight.

The high-frequency X and Y angle random errors are strongly correlated. Approximately 30 plots of X and Y angle autocorrelation functions have been supplied by Goddard Space Flight Center. These plots have been reduced to analytical form as shown below. For the X angle noise

$$\phi_j / \phi_0 = e^{-j\Delta T / 2.58} \left[\cos \left(\frac{360 j \Delta T}{5.16} \right)^\circ - 0.3185 \sin \left(\frac{360 j \Delta T}{5.16} \right)^\circ \right] \quad (22)$$

where $\phi_0 = \sigma_{qX}^2$. For the Y angle noise

$$\phi_j / \phi_0 = e^{-j\Delta T / 1.80} \left[\cos \left(\frac{360 j \Delta T}{4.87} \right)^\circ - 0.4304 \sin \left(\frac{360 j \Delta T}{4.87} \right)^\circ \right] \quad (23)$$

where $\phi_0 = \sigma_{qY}^2$. Figure 1 shows plots of the X and Y angle autocorrelation functions.

Simulated data having the above autocorrelation functions can be generated by (ref. 10)

$$\epsilon_i = a_1 \epsilon_{i-1} - a_2 \epsilon_{i-2} + b_1 \eta_i + b_2 \eta_{i-1} \quad (24)$$

where

$$E(n_i) = 0$$

$$E(n_i n_j) = \begin{cases} 0 & \text{for } i \neq j \\ 1 & \text{for } i = j \end{cases}$$

$$a_1 = \frac{\phi_3/\phi_0 - (\phi_2/\phi_0)(\phi_1/\phi_0)}{\phi_2/\phi_0 - (\phi_1/\phi_0)^2} \quad (25)$$

$$a_2 = \frac{(\phi_1/\phi_0)(\phi_3/\phi_0) - (\phi_2/\phi_0)^2}{\phi_2/\phi_0 - (\phi_1/\phi_0)^2} \quad (26)$$

$$\begin{aligned} b_1/\sqrt{\phi_0} = & 1/2 \sqrt{1 - a_1 + a_2} \sqrt{1 - a_1 - a_2 + 2\phi_1/\phi_0} \\ & + 1/2 \sqrt{1 + a_1 + a_2} \sqrt{1 + a_1 - a_2 - 2\phi_1/\phi_0} \end{aligned} \quad (27)$$

$$\begin{aligned} b_2/\sqrt{\phi_0} = & 1/2 \sqrt{1 - a_1 + a_2} \sqrt{1 - a_1 - a_2 + 2\phi_1/\phi_0} \\ & - 1/2 \sqrt{1 + a_1 + a_2} \sqrt{1 + a_1 - a_2 - 2\phi_1/\phi_0} \end{aligned} \quad (28)$$

For example, if $\Delta T = 0.2$ seconds, then the simulated X angle noise is generated by

$$\epsilon_i = 1.7962\epsilon_{i-1} - 0.8564\epsilon_{i-2} + \sigma_{qX}(0.5156n_i - 0.5057n_{i-1}) \quad (29)$$

Y angle noise is generated by

$$\epsilon_i = 1.7305\epsilon_{i-1} - 0.8009\epsilon_{i-2} + \sigma_{qY}(0.5976n_i - 0.5846n_{i-1}) \quad (30)$$

If $\Delta T = 0.05$ seconds, X angle noise is generated by

$$\epsilon_i = 1.958\epsilon_{i-1} - 0.962\epsilon_{i-2} + 0.2729\sigma_{qX}(n_i - n_{i-1}) \quad (31)$$

and $\phi_1/\phi_0 = 0.96$, $\phi_i/\phi_0 = 1.958\phi_{i-1}/\phi_0 - 0.962\phi_{i-2}/\phi_0$. The Y angle noise is generated by

$$\epsilon_i = 1.9412\epsilon_{i-1} - 0.9460\epsilon_{i-2} + 0.3240\sigma_{qY}(\eta_i - \eta_{i-1}) \quad (32)$$

and $\phi_1/\phi_0 = 0.9436$, $\phi_i/\phi_0 = 1.9412\phi_{i-1}/\phi_0 - 0.9460\phi_{i-2}/\phi_0$.

The recommended high-frequency noise standard deviations for S-band data are summarized below.

$$\begin{array}{lll} \sigma_{q\phi H} = 3.3 \text{ m} & \sigma_{q\phi H, MAX} = 10 \text{ m (3}\sigma) & \sigma_{q\phi H, MIN} = 0.24 \text{ m} \\ \sigma_{qXH} = 0.15 \text{ mrad} & \sigma_{qXH, MAX} = 0.40 \text{ mrad} & \sigma_{qXH, MIN} = 0.03 \text{ mrad} \\ \sigma_{qYH} = 0.09 \text{ mrad} & \sigma_{qYH, MAX} = 0.16 \text{ mrad} & \sigma_{qYH, MIN} = 0.04 \text{ mrad} \\ \sigma_{qDH} = 4 \text{ mm} = 60 \text{ cycles} & & \\ \sigma_{qDH, MAX} = 12.7 \text{ mm} = 190 \text{ cycles} & & \\ \sigma_{qDH, MIN} = 0.8 \text{ mm} = 12 \text{ cycles} & & \\ \sigma_{qDH} = 24 \text{ mm} = 360 \text{ cycles for HAW3} & & \end{array}$$

$$\begin{array}{l} \sigma_{q\phi S} = 0.005 \text{ m} \\ \sigma_{qAS} = 0.15 \text{ mrad} \\ \sigma_{qES} = 0.5 \text{ mrad} \\ \sigma_{qDS} = 5 \text{ mm} = 75 \text{ cycles} \end{array}$$

The bias error statistics due to hardware were obtained from references 13, 14, 15, 16 and 17.

$$\begin{array}{lll} \sigma_{B\phi H} = 28 \text{ m} & \sigma_{B\phi H, MAX} = 61 \text{ m} & \sigma_{B\phi H, MIN} = 18 \text{ m} \\ \sigma_{BXH} = 0.5 \text{ mrad} & \sigma_{BXH, MAX} = 1.85 \text{ mrad}^a & \sigma_{BXH, MIN} = 0.10 \text{ mrad}^a \\ \sigma_{BYH} = 0.25 \text{ mrad} & \sigma_{BYH, MAX} = 1.66 \text{ mrad}^a & \sigma_{BYH, MIN} = 0.19 \text{ mrad}^a \\ \sigma_{BDH} = 7.5 \text{ Hz} & \sigma_{BDH, MIN} = 10 \text{ Hz} & \sigma_{BDH, MIN} = 5 \text{ Hz} \\ = 0.5 \text{ mm/sec} & = 0.67 \text{ mm/sec} & = 0.33 \text{ mm/sec} \end{array}$$

Reference 16 states that the Doppler (rate) bias error should be modeled as an exponentially correlated random variable adding to the Doppler constant of integration. The time constant is less than 400 seconds.

Refraction correction errors increase the hardware bias standard deviations at low-elevation angles in the following way.

$$\sigma_{B\phi} = \sqrt{\sigma_{B\phi H}^2 + \sigma_{B\phi N}^2 + \sigma_{B\phi A}^2} \quad (33)$$

$\sigma_{B\phi N}$ is given by equation 4 and is the error due to the error in the modulus of refraction N_0 at the observer (station). $\sigma_{B\phi A}$ is due to algorithm errors in computing the refraction correction $\Delta\phi$. Both $\sigma_{B\phi N}$ and $\sigma_{B\phi A}$ should be small compared to the recommended value for $\sigma_{B\phi H} = 28$ meters.

^aFor an uncalibrated station.

The total X and Y angle bias standard deviations are

$$\sigma_{BX} = \sqrt{\sigma_{BXH}^2 + \left(\frac{\partial \alpha_X}{\partial E}\right)^2 (\sigma_{BEN}^2 + \sigma_{BEA}^2)} \quad (34)$$

$$\sigma_{BY} = \sqrt{\sigma_{BYH}^2 + \left(\frac{\partial \alpha_Y}{\partial E}\right)^2 (\sigma_{BEN}^2 + \sigma_{BEA}^2)} \quad (35)$$

σ_{BEN} is the error due to errors in N_0 and is given by equation 5. σ_{BEA} is due to the algorithm error in computing ΔE and is a function of the algorithm used.

4.0 REFERENCES

1. Eastern Test Range Quarterly Accuracy Report No. 61. RCA International Service Corporation, Patrick Air Force Base, Florida, March 30, 1977.
2. Eastern Test Range Quarterly Accuracy Report No. 63. RCA International Service Corporation, Patrick Air Force Base, Florida, September 30, 1977.
3. Eastern Test Range Quarterly Accuracy Report No. 64. RCA International Service Corporation, Patrick Air Force Base, Florida, December 30, 1977.
4. Systems Performance and Accuracy Report. Space and Missile Test Center, Air Force Systems Command, Vandenberg Air Force Base, California 93437, May 1977.
5. Station Characteristics for Apollo Mission Support. Flight Software Branch/Flight Support Division, NASA/JSC, May 1967.
6. Lear, William M.: Refraction Corrections for An Exponential Atmosphere. Johnson Space Center Internal Note 75-FM-60, August 18, 1975.
7. Lear, William M.: High-Precision Refraction Correction Algorithms. Johnson Space Center Internal Note 78-FM-44, August 1978.
8. Lear, William M.: Orbital Refraction Corrections For Range And Elevation Angle. JSC Memorandum FM82(79-185), May 29, 1979.
9. Telephone conversation with Lee Eckes of TRW, One Space Park, Redondo Beach, California. February 1979.
10. Lear, William M.: Kalman Filtering Techniques. NASA/JSC Internal Note 78-FM-28, April 1978.
11. Pixley, Paul T.: S-Band Transponder Design and Range Measurements. JSC Memorandum FM82(79-176), May 17, 1979.
12. Jackson, J. A.: STDN Metric Tracking Data Evaluation Report for July 1976. Goddard Space Flight Center Report, STDN No. 720/July 1976.
13. Jackson, J. A.: STDN Metric Tracking Data Evaluation Report for July 1977. Goddard Space Flight Center Report, STDN No. 720/July 1977.
14. Jackson, J. A.: STDN Metric Tracking Data Evaluation Report for February 1978. Goddard Space Flight Center Report, STDN No. 720/February 1978.
15. Jackson, J. A.: S-Band Tracker Performance, Low-Speed Data. Handout at February 1979 DOWG meeting.
16. Lear, William M.: Mathematical Models For Short Range Data From A Single S-Band Station. JSC Internal Note 76-FM-66, August 25, 1976.

17. Hogan, Michael C.: STDN Angle Accuracy Improvement. Handout at June DOWG meeting at White Sands Missile Range, New Mexico.

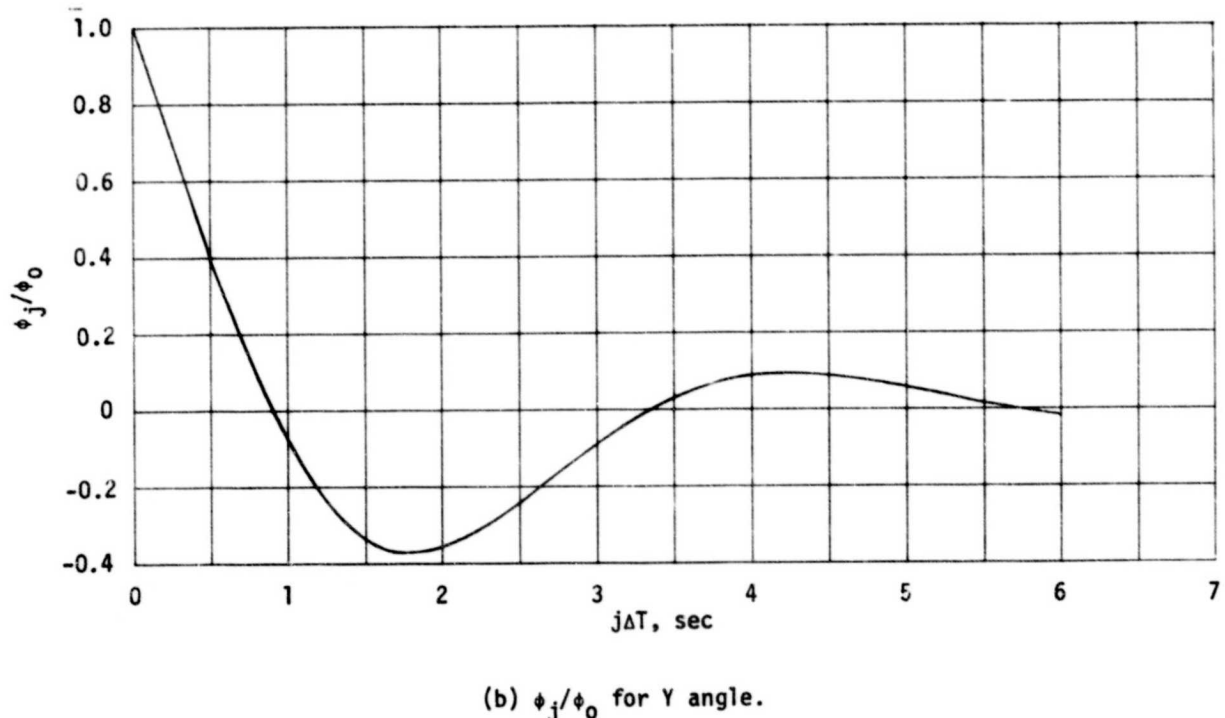
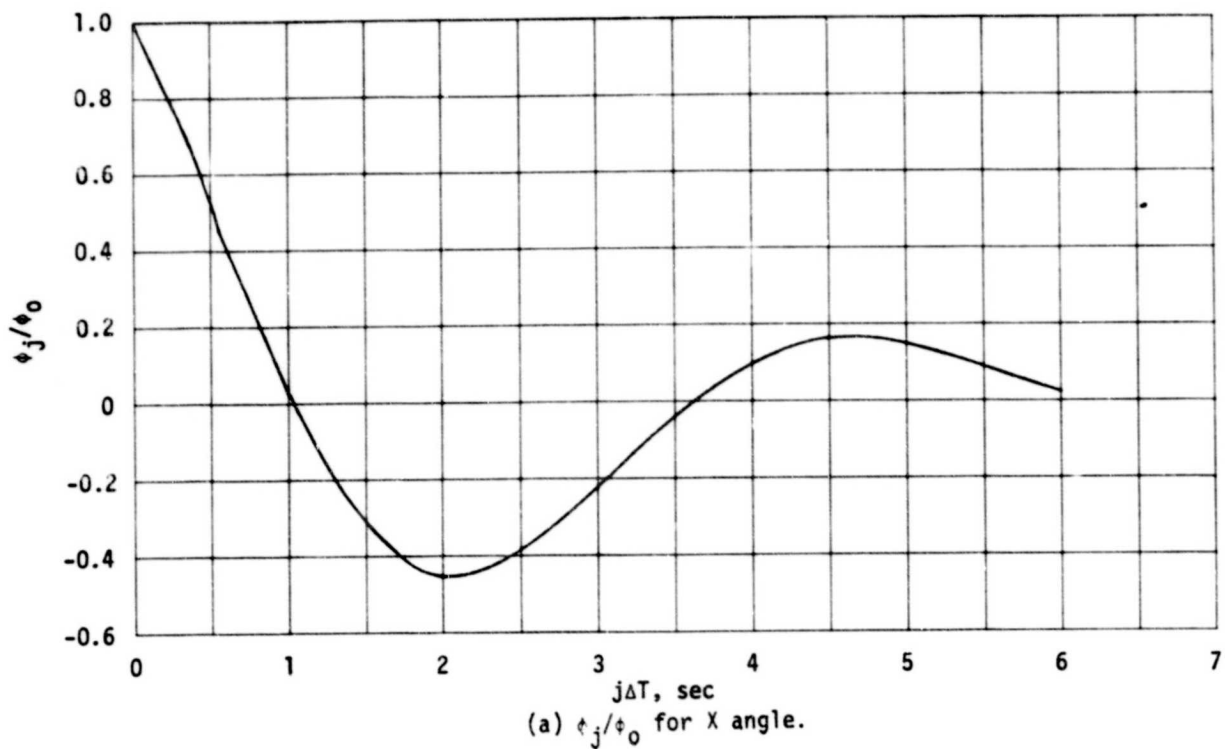


Figure 1.- Normalized auto correlation functions.